THE JOURNAL OF PHYSICAL CHEMISTRY C
A JOURNAL OF THE AMERICAN CHEMICAL SOCIETY

pubs.acs.org/JPCC

Article

Chemical Reactions in Imperfect Cavities: Enhancement, Suppression, and Resonance

John P. Philbin,* Yu Wang,* Prineha Narang,* and Wenjie Dou*

Cite This: https://doi.org/10.1021/acs.jpcc.2c04741

Read Online

ACCESS | Metrics & More | Article Recommendations

ABSTRACT: The use of optical cavities to control chemical reactions has been of great interest recently, following demonstrations of enhancement, suppression, and negligible effects on chemical reaction rates depending on the specific reaction and cavity frequency. In this work, we study the reaction rate inside imperfect cavities, where we introduce a broadening parameter in the spectral density to mimic Fabry−Pérot cavities. We investigate cavity modifications to reaction rates using non-Markovian Langevin dynamics with frictional and random forces to account for the presence of imperfect optical cavities. We demonstrate that, in the regime of weak solvent and cavity friction, the cavity can enhance chemical reaction rates. On the other hand, in the high friction regime, cavities can suppress chemical reactions. Furthermore, we find that the broadening of the cavity spectral density gives rise to blue shifts of the resonance conditions and, surprisingly, increases the sharpness of the resonance effect.

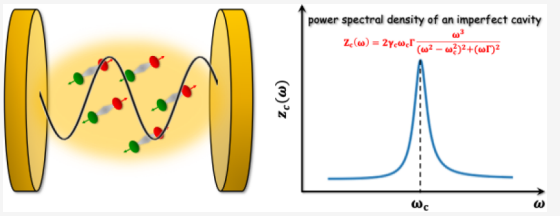

I. INTRODUCTION

The concept of selectively controlling the rate of a chemical reaction by shining light in resonance with a specific molecular bond has been explored for many decades. Two drawbacks of this scheme are that it requires light energy as an input and, arguably more importantly, molecular bonds often quickly transfer the vibrational energy in the mode of interest to other vibrations and degrees of freedom. A possible way to circumvent these two obstacles is to tune the frequencies of an optical cavity to selectively alter the ground state chemical reactivity of molecules, which was demonstrated recently experimentally.[1−3] This research avenue has attracted many experimental,[4−7] computational,[8−16] and theoretical[17−20] investigations in recent years as which reactions can be manipulated by optical cavities and the underlying mechanism of how cavities can modify chemical reactivity are still an open questions.[21−23]

In this work, we study the reaction rate inside an optical cavity by developing a non-Markovian dynamical model. The effect of the cavity mode on the reaction mode dynamics is incorporated into friction and random forces.[24,25] This model allows us to continuously model Fabry−Pérot cavities from their ideal perfect single mode cavity limit to more realistic lossy, imperfect cavities (Figure 1).[26] In Kramer's theory dealing with Ohmic friction, the rate of escape of a particle over a potential barrier increases linearly with increasing friction in the underdamped limit and decreases inversely with the friction strength in the strong damping limit.[27] Grote and Hynes proceeded to solve the Kramer's rate problem in the presence of memory friction, in the regime of moderate to strong friction.[28] The continuum limit version of Kramer's theory that covers the whole range of friction is known as Pollak, Grabert, and Hänggi (PGH) theory.[29] To cover the whole range of friction, our numerical and analytical analysis show that optical cavities can both enhance or suppress chemical reaction rates, depending on the magnitude of the solvent friction as well as the cavity-molecule coupling strength. This reaction rate enhancement in the weak friction regime and suppression in the strong friction regime was also reported in a recent computational study[30] and a PGH theory-based study[31] for perfect cavities. Our work, developed concurrently and independently of these studies, is in agreement with these works and also allows the inclusion of cavity imperfectness through a broadened spectral density of the non-Markovian cavity bath. Interestingly, we find that increasing the cavity-molecule coupling strength gives rise to a red shift of the

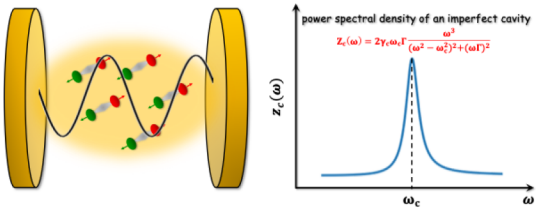

Figure 1. Schematic representation of light−matter vibrational strong coupling in an imperfect cavity, and the spectra density of the cavity.

Received: July 5, 2022
Revised: July 28, 2022

cavity frequency that has the greatest impact on the reaction rate (i.e., red shift of the resonance condition) whereas making the cavity more imperfect by increasing the broadening parameter of the cavity spectral density results in a blue shift of the resonance condition and also sharpens the resonance condition.

The manuscript is organized as follows. In Section II, we introduce our model and derive the Langevin dynamics for the molecules in the presence of a Markovian phonon bath and non-Markovian cavity mode. In Section III, we perform both numerical and analytical analysis to obtain cavity-modified chemical reaction rates within our model. Lastly, we conclude in Section IV.

II. THEORY

Here, we consider the reaction mode to be a one-dimensional double well potential energy surface (PES). The reaction mode couples to a set of harmonic oscillators corresponding to the solvent environment as well as a set of harmonic oscillators corresponding to the optical cavity. The total Hamiltonian that we utilize is given by the Pauli-Fierz nonrelativistic quantum electrodynamics (QED) Hamiltonian in the dipole gauge and in the long-wavelength limit:[32,33]

$$H = \frac{p^2}{2m} + V(x) + \frac{1}{2}\sum_j m_j\left[\dot{q}_j^2 + \omega_j^2(q_j + c_j x)^2\right] + \frac{1}{2}\sum_k \left[P_k^2 + \tilde{\omega}_k^2(Q_k + \mu_k x)^2\right] \tag{1}$$

Here, x and p are the coordinates for the reaction mode, q_j and $\dot{q}_j$ are the coordinates for the other vibrational modes that will compose the Markovian bath, Q_k and P_k are the coordinates for the cavity modes that will compose the non-Markovian bath, c_j and μ_k are coupling strengths of the reaction coordinates to the vibrational bath modes and cavity modes. The double well PES for the reaction mode is given by[34]

$$V(x) = \frac{1}{2}m\omega_0^2 x^2 - a\cdot\log(1 + e^{-(gx\sqrt{2m\omega_0/\hbar} + E_d)/a}) \tag{2}$$

where $\omega_0 = 0.003$, $a = 0.02$, $g = 0.02$, $E_d = 4/30$ are the parameters used in our calculations below, and we set $\hbar = 1$ throughout this work. In the semiclassical limit, we can write down the equation of motion for the reaction mode as

$$m\ddot{x} = -\frac{\mathrm{d}V}{\mathrm{d}x} - \sum_j m_j\omega_j^2(c_j q_j + c_j^2 x) - \sum_k \tilde{\omega}_k^2(\mu_k Q_k + \mu_k^2 x) \tag{3}$$

Similarly, we can also write down the equations of motion for the vibrational bath modes and cavity modes

$$m_j\ddot{q}_j = -m_j\omega_j^2 q_j - m_j\omega_j^2 c_j x \tag{4}$$

$$\ddot{Q}_k = -\tilde{\omega}_k^2 Q_k - \tilde{\omega}_k^2\mu_k x \tag{5}$$

Because the above equations are linear, they can be solved explicitly:[35]

$$q_j(t) = q_{j0}\cos(\omega_j t) + \frac{\dot{q}_{j0}}{\omega_j}\sin(\omega_j t) - c_j x(t) + c_j\int_0^t \mathrm{d}\tau\ \cos(\omega_j(t-\tau))\dot{x}(\tau) \tag{6}$$

where q_{j0} and $\dot{q}_{j0}$ are the initial position and momenta for the solvent environment. We can solve for P_k, Q_k in a similar manner,

$$Q_k(t) = Q_{k0}\cos(\tilde{\omega}_k t) + \frac{\dot{Q}_{k0}}{\tilde{\omega}_k}\sin(\tilde{\omega}_k t) - \mu_k x(t) + \mu_k\int_0^t \mathrm{d}\tau\ \cos(\tilde{\omega}_k(t-\tau))\dot{x}(\tau) \tag{7}$$

If we plug in eqs 6 and 7 into the equation of motion for x given by eq 3, we find a generalized Langevin equation:

$$m\ddot{x} = -\frac{\mathrm{d}V}{\mathrm{d}x} - \int_0^t \mathrm{d}\tau(Z_p(t-\tau) + Z_c(t-\tau))\dot{x}(\tau) + R_p(t) + R_c(t) \tag{8}$$

where

$$Z_p(t) = \sum_j m_j\omega_j^2 c_j^2\cos(\omega_j t) \tag{9}$$

$$Z_c(t) = \sum_k \tilde{\omega}_k^2\mu_k^2\cos(\tilde{\omega}_k t) \tag{10}$$

$$R_p(t) = -\sum_j m_j\omega_j^2 c_j\left(q_{j0}\cos(\omega_j t) + \frac{\dot{q}_{j0}}{\omega_j}\sin(\omega_j t)\right) \tag{11}$$

$$R_c(t) = -\sum_k \tilde{\omega}_k^2\mu_k\left(Q_{k0}\cos(\tilde{\omega}_k t) + \frac{\dot{Q}_{k0}}{\tilde{\omega}_k}\sin(\tilde{\omega}_k t)\right) \tag{12}$$

Here $R_p(t)$ and $R_c(t)$ are random forces from the phonon bath and cavity, respectively, and $Z_c(t)$ and $Z_p(t)$ are the corresponding friction kernels. Below we consider the case that friction and random forces from the phonon environments are Markovian, such that the Langevin equation can be simplified as

$$m\ddot{x} = -\frac{\mathrm{d}V}{\mathrm{d}x} - \int_0^t \mathrm{d}\tau Z_c(t-\tau)\dot{x}(\tau) + R_c(t) - \gamma_p\dot{x}(t) + R_p(t) \tag{13}$$

We now turn our attention to the frictional force from the cavity. We consider the spectral density with broadening parameters in an imperfect cavity.[26] In particular, the spectral density is taken to the form of a Cauchy distribution to mimic a Fabry–Pérot cavity:

$$Z_c(\omega) = 2\gamma_c\omega_c\Gamma\frac{\omega^3}{(\omega^2 - \omega_c^2)^2 + (\omega\Gamma)^2} \tag{14}$$

In eq 14, γ_c quantifies the coupling strength of the reaction coordinate to the cavity, ω_c corresponds to the center frequency where the cavity density of states is largest (and is the frequency of the one cavity mode in the perfect cavity scenario), and Γ is the broadening parameter that determines the extent to which the cavity is imperfect (i.e., lossy). As $\Gamma \to 0$, $Z_c(\omega)$ approaches a δ-function, reflecting a perfect cavity.

The memory kernel is then given by

$$Z_c(t) = \frac{2}{\pi}\int_0^\infty \frac{Z_c(\omega)}{\omega}\cos(\omega t)\ \mathrm{d}\omega \tag{15}$$

The solution of the cavity memory kernel in the time domain has two solutions, depending on the cavity center frequency and broadening. When $\omega_c > \Gamma/2$, the cavity memory kernel is

$$Z_c(t) = 2\gamma_c\omega_c e^{-\frac{\Gamma t}{2}}\left(\frac{\cos(\omega_1 t)}{2} - \frac{\Gamma\sin(\omega_1 t)}{4\omega_1}\right) \tag{16}$$

where we defined $\omega_1 = \sqrt{\omega_c^2 - \Gamma^2/4}$. And when $\omega_c < \Gamma/2$, the cavity memory kernel is

https://doi.org/10.1021/acs.jpcc.2c04741
J. Phys. Chem. C XXXX, XXX, XXX−XXX

$$Z_c(t) = 2\gamma_c\omega_c e^{-\frac{\Gamma t}{2}}\left(\frac{\cosh(\omega_1 t)}{2} - \frac{\Gamma \sinh(\omega_1 t)}{4\omega_1}\right) \quad (17)$$

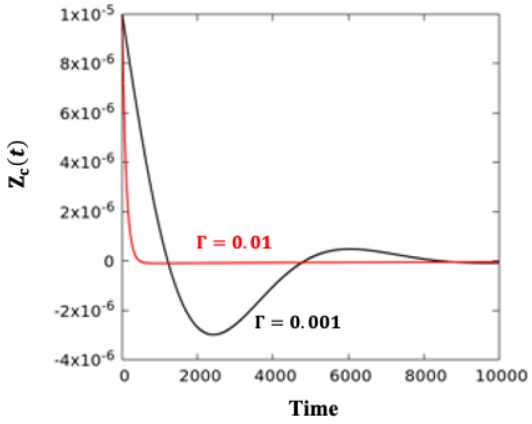

Figure 2. Memory kernel $Z_c(t)$ as a function of time with a small Γ (black line) and a large Γ (red line). The other model parameters used here are $\gamma_c = 0.01$ and $\omega_c = 0.001$.

with $\omega_1 = \sqrt{\Gamma^2/4 - \omega_c^2}$. As shown in Figure 2, the cavity memory kernel in the time domain converges toward a δ-function as Γ increases, whereas, when Γ approaches to 0, the memory kernel will oscillate as a cosine function. The cavity random force $R_c(t)$ is related to the memory kernel $Z_c(t)$ via the fluctuation−dissipation theorem:

$$\langle R_c(0)R_c(t)\rangle = mk_BTZ_c(t) \quad (18)$$

Note that the time correlation function of the random force is non-Markovian. To generate such non-Markovian random force, we propagate the following equations of motion:

$$\dot{Y} = \omega_c R_c \quad (19)$$

$$\dot{R}_c = -\omega_c Y - \Gamma R_c + \sqrt{\omega_c\Gamma}\,\xi(t) \quad (20)$$

Here, $\xi(t)$ is a Markovian random variable from a Gaussian distribution with a standard deviation of $\sigma = \sqrt{2m\gamma_c k_B T/dt}$, where dt is the time step interval. Y is an auxiliary variable. We can show that, in the long time limit, the above equations generate R_c that satisfies the correlation function in eq 18.

As for the solvent (i.e., vibrational) bath, the random force $R_p(t)$ is Markovian ($\langle R_p(0)R_p(t)\rangle = 2mk_BT\gamma_p\delta(t)$), which is set to be a Gaussian random variable with a standard deviation of $\sigma_p = \sqrt{2m\gamma_p k_B T/dt}$. We use fourth-order Runge−Kutta to integrate eqs 13, 19, and 20. Lastly, unless stated otherwise, we perform thermal averages over 10000 trajectories in our non-Markovian Langevin dynamics simulations.

III. RESULTS AND DISCUSSION

We first investigate cavity modified reaction rates in the weak solvent friction regime, namely, when γ_p is small. We calculate the reaction rates by initializing all trajectories in the reactant well with a Boltzmann distribution and monitoring the number of trajectories that end up in the product well as a function of time by numerically solving the non-Markovian Langevin dynamics, as illustrated in Figure 3. We find that, with a fixed photon frequency $\omega_c = 0.005$, a turnover occurs in the chemical

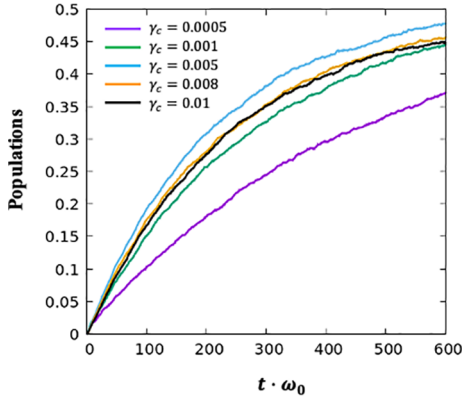

Figure 3. Product populations as a function of time t with different cavity friction γ_c, calculated by non-Markovian Langevin dynamics. The other model parameters used here are $\omega_0 = 0.003$, $\omega_b = 0.007$, barrier height $E_b = 0.0195$, $\gamma_p = 0.00001$, $\omega_c = 0.005$, $k_BT = 0.005$, $\Gamma = 0.01$.

reaction rate as a function of the cavity friction γ_c. Specifically, we find that initially increasing the cavity friction results in an increase in the reaction rate but, eventually, increasing the cavity friction leads to a decrease in the reaction rate. This turnover is the well-known Kramer's turnover, which occurs in the overdamped regime.[36] Therefore, with small solvent friction, the Kramer turnover effect can be observed here as a function of the cavity friction.

We then proceed to investigate the reaction rate as a function of the cavity frequency, where the rate is extracted by exponentially fitting the product population as a function of time. In the limit of weak solvent friction, we see that the cavity can enhance reaction rates ($\omega_c \approx \omega_0$) (Figure 4). The maximum

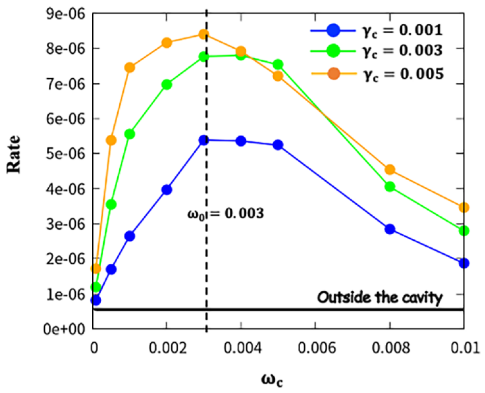

Figure 4. Cavity-modified reaction rate as a function of the cavity photon frequency ω_c at three different cavity friction values, $\gamma_c = 0.001$, 0.003, and 0.005, calculated by non-Markovian Langevin dynamics. The black line is the reaction rate outside the cavity. The other model parameters used here are $\omega_0 = 0.003$, $\omega_b = 0.007$, barrier height $E_b = 0.0195$, $\gamma_p = 0.00001$, $k_BT = 0.005$, and $\Gamma = 0.01$.

cavity-modified reaction rate enhancement occurs at a cavity frequency around the vibrational frequency of the reactant well ($\omega_0 = 0.003$, Figure 4). Upon increasing the cavity friction γ_c from 0.001 to 0.005, the cavity enhances the reaction even more as the total friction remains in the underdamped regime. Further

https://doi.org/10.1021/acs.jpcc.2c04741
J. Phys. Chem. C XXXX, XXX, XXX−XXX

increasing the cavity friction will eventually result in suppressing chemical reactions as shown in Figure 3 (overdamped regime).

We now turn our focus to the strong solvent friction regime, namely, when γ_p is large. In this regime, the reaction rates are monotonically suppressed upon increasing the cavity friction, which is in agreement with Grote−Hynes (GH) theory.[7,19,28] In this limit, the reaction rate is given by

$$k = \kappa_{GH} k_{TST} \tag{21}$$

Here $k_{TST} = \frac{\omega_0}{2\pi} e^{-\beta E_b}$ is the transition state theory rate, where $E_b = V(-E_d/(g\sqrt{2m\omega_0/\hbar})) - V(0) \approx 0.0195$ is the potential energy barrier. κ_{GH} is the Grote−Hynes transmission coefficient. We can employ an analytical approach for calculating κ_{GH} to understand how cavities can modify chemical reactions in this regime as a function of the cavity frequency, ω_c. Particularly, the GH coefficient is given by

$$\lambda^2 = \omega_b^2 - \lambda \cdot (\tilde{\xi}_c(\lambda) + \tilde{\xi}_p(\lambda)) \tag{22}$$

where $\tilde{\xi}_c(\lambda)$ and $\tilde{\xi}_p(\lambda)$ are the Laplace transformed cavity photon friction and solvent vibrational bath friction, respectively. Using the spectral density $Z_c(\omega)$, one can write $\tilde{\xi}_c(\lambda)$ as

$$\tilde{\xi}_c(\lambda) = \frac{2}{\pi} \int_0^\infty \frac{Z_c(\omega)}{\omega} \frac{\lambda}{\lambda^2 + \omega^2} d\omega \tag{23}$$

For solvent bath friction, we have $\tilde{\xi}_p = \gamma_p$. GH coefficient is then obtained from $\kappa_{GH} = \lambda/\omega_b$.

In Figure 5 we plot κ_{GH} as a function of ω_c analytically. The two green lines show reaction rates for two perfect cavities with

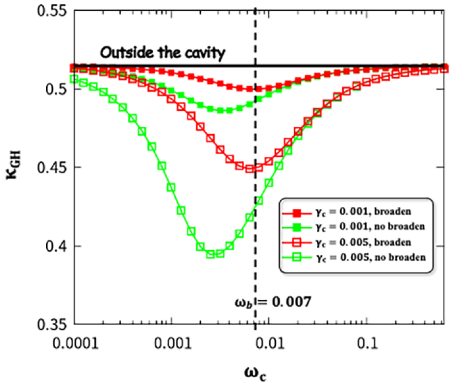

Figure 5. Cavity-modified transmission coefficient κ_{GH} for the reaction rate as a function of the cavity photon frequency ω_c at different cavity frictions γ_c = 0.001, 0.005. The black line is the κ_{GH} outside the cavity. The other model parameters used here are ω_0 = 0.003, ω_b = 0.007, barrier height E_b = 0.0195, γ_p = 0.01, and $k_B T$ = 0.005, for the green lines, Γ = 0.0001, and for the red lines, Γ = 0.01.

different cavity frictions (γ_c) in comparison to two red lines that show reaction rates for imperfect cavities (i.e., cavities with broadened spectral densities) with all other parameters held constant. In agreement with recent reports,[7,19] when the cavity friction (γ_c) is small, the minimum of κ_{GH} appears at a cavity frequency close to the barrier frequency, ω_b = 0.007. Upon increasing γ_c, the cavity frequency corresponding to the minimum of κ_{GH} is shifted to lower energies (i.e., the resonance condition is red-shifted). This red shift of the resonance condition upon increasing coupling to the cavity in the strong friction regime agrees well with recent findings[7,19] and, interestingly, competes with the impact that broadening the cavity spectral density has on the resonance condition. Specifically, Figure 5 also shows the effect of imperfect cavities on the resonance conditions. We see that the cavity frequency with greatest impact on the reaction rates is shifted to higher energies (i.e., blue-shifted) upon increasing the cavity imperfectness. This is demonstrated in Figure 5 by observing that the maximum rate suppression occurs at higher cavity frequencies for the imperfect cavities (red lines) compared to the corresponding perfect cavities (green lines). Additionally, the resonance condition surprisingly sharpens in the case of a broadened cavity spectral density, especially on the low frequency side of the maximum rate suppression. Furthermore, we see that the imperfectness reduces the efficiency of the cavity on chemical reactivity. Such a finding is different from the results shown in ref 7, where the authors found that increasing the cavity loss rate increases the cavity impact on reaction rate. Note that we are using a different model to introduce cavity imperfectness than used in ref 7.

To understand the red and blue shifts, we examine the GH theory again. To simplify the analysis here, we eliminate the friction from phonon bath. In the limit of Γ = 0 (perfect cavity), the GH equation becomes

$$\lambda^2 = \omega_b^2 - 2\gamma_c \omega_c \frac{\lambda^2}{\lambda^2 + \omega_c^2} \tag{24}$$

We can solve for ω_c where we reach minimum κ_{GH} by finding the solution $\partial\lambda/\partial\omega_c = 0$ (see the Appendix):

$$\omega_c = -\frac{\gamma_c}{2} + \sqrt{\frac{\gamma_c^2}{4} + \omega_b^2} \approx \omega_b - \frac{\gamma_c}{2} \tag{25}$$

Here, we have expanded the above result to first order in γ_c. Clearly, the coupling strength γ_c will introduce a red shift for the resonance condition $\omega_c = \omega_b$, in agreement with findings reported recently in ref 19. We can also extend the analysis of ref 19 to the case of an imperfect cavity.

For the imperfect cavity with nonzero Γ, we can introduce a factor Q to approximate the following integral

$$\frac{2}{\pi} \int_0^\infty \frac{\Gamma\omega^2}{(\omega^2 - \omega_c^2)^2 + (\omega\Gamma)^2} \frac{\lambda}{\lambda^2 + \omega^2} d\omega = \frac{\lambda}{\lambda^2 + (Q\omega_c)^2} \tag{26}$$

In the limit Γ = 0, we have Q = 1. Such that we recover the results for the perfect cavity. The nonzero Γ will lead to Q < 1 for an imperfect cavity. The minimum κ_{GH} is then located at

$$\omega_c = \frac{1}{Q^2}\left(-\frac{\gamma_c}{2} + \sqrt{\frac{\gamma_c^2}{4} + \omega_b^2}\right) \tag{27}$$

Since Q < 1, the broadening will give rise to a blue shift.

In Figure 6, we further verify the effects of broadening on the transmission coefficient κ_{GH} as a function of the cavity frequency ω_c using numerical and analytic methods. Specifically, the green lines and red lines utilize the analytic expressions for a perfect and imperfect cavity, respectively and the black lines are the numerical results obtained from the full non-Markovian Langevin dynamics with the same Γ as the red lines. Figure 6a shows that when Γ is small, there is no broadening effect in the spectral density of the cavity mode such that these three methods predict the same κ_{GH} for all values of ω_c. In particular, κ_{GH} exhibits a minimum when the cavity frequency is close to the barrier frequency (ω_b = 0.007). On the other hand, for the

https://doi.org/10.1021/acs.jpcc.2c04741
J. Phys. Chem. C XXXX, XXX, XXX−XXX

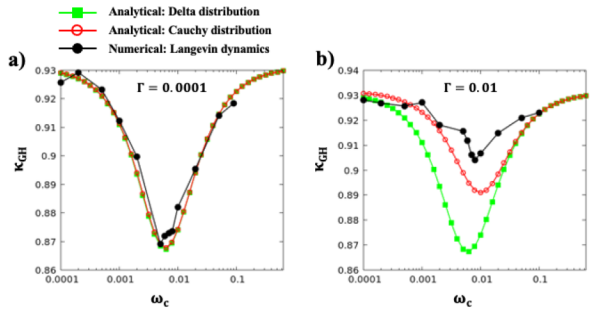

Figure 6. Cavity-modified transmission coefficient κ_{GH} for the reaction rate as a function of photon frequency ω_c for (a) a perfect cavity (Γ = 0.0001) and (b) an imperfect cavity (Γ = 0.01). The other model parameters used here are ω_0 = 0.003, ω_b = 0.007, barrier height E_b = 0.0195, k_BT = 0.005, γ_p = 0.001, γ_c = 0.001.

relatively larger Γ value shown in Figure 6b, the broadening effect of the cavity spectral density leads to a blue shift in the frequency at which the cavity has the largest impact on the reaction rate, and the width of the resonance narrows. This observation is in agreement with our analytical analysis above. Furthermore, the broadening effects tend to reduce the efficiency of the cavity mode on the reaction rate. With a very large Γ, we expect that the cavity will not affect the chemical reaction at all.

IV. CONCLUSIONS

We developed a non-Markovian friction and random force model to study how imperfect optical cavities can modify chemical reaction rates. We found that in the small solvent friction regime, cavities can enhance chemical reaction rates while in the large solvent friction regime cavities suppress reactions. We also reported that imperfect cavities have resonance conditions that are both shifted to higher frequencies and sharper relative to otherwise identical perfect cavities.

After completing this work, we noticed that two similar results were reported in the literature.[30,31] Our work is in agreement with these findings and differentiates itself from those works as we investigated the effect of imperfect cavities, both numerically and analytically, on chemical reaction rates while the other reports focused on perfect cavities.

APPENDIX

As stated in the main text, to simplify the analysis in the large friction regime, we eliminate the friction from phonon bath. In the limit of Γ = 0 (perfect cavity), we have

$$\lambda^2 = \omega_b^2 - 2\gamma_c\omega_c\frac{\lambda^2}{\lambda^2 + \omega_c^2} \tag{A.1}$$

When $\frac{\partial\lambda}{\partial\omega_c} = 0$ we have a relation between λ_{min} and ω_c as

$$\lambda_{min^2} = \frac{\omega_b^2}{1 + \frac{\gamma_c}{\omega_c}} \tag{A.2}$$

Substituting eq A.2 into eq A.1 we could get a relationship as follows

$$\lambda_{min} = \omega_c \tag{A.3}$$

Substituting eq A.3 into eq A.2, we obtain a function relating to the ω_c that corresponding to the λ_{min} (i.e., the minimum of κ_{GH})

$$\omega_c^2 + \gamma_c\omega_c - \omega_b^2 = 0 \tag{A.4}$$

When solving the above equation, we get

$$\omega_c = -\frac{\gamma_c}{2} + \sqrt{\frac{\gamma_c^2}{4} + \omega_b^2} \tag{A.5}$$

It is evident that when increasing the γ_c, the ω_c corresponding to the minimum κ_{GH} will red shift.

For the imperfect cavity, when introducing a Q factor, the GH equation becomes

$$\lambda^2 = \omega_b^2 - 2\gamma_c\omega_c\frac{\lambda^2}{\lambda^2 + (Q\omega_c)^2} \tag{A.6}$$

When $\frac{\partial\lambda}{\partial\omega_c} = 0$, we have a relation between λ_{min} and ω_c as

$$\lambda_{min^2} = \frac{\omega_b^2}{1 + \frac{\gamma_c}{Q^2\omega_c}} \tag{A.7}$$

Substituting eq A.7 into eq A.6, we could obtain

$$\lambda_{min} = Q\omega_c \tag{A.8}$$

Substituting eq A.8 into eq A.7 gets a function relating to the ω_c that corresponds to the λ_{min} in the imperfect cavity

$$Q^2\omega_c^2 + \gamma_c\omega_c - \omega_b^2 = 0 \tag{A.9}$$

When solving the above equation, we obtain

$$\omega_c = \frac{1}{Q^2}\left(-\frac{\gamma_c}{2} + \sqrt{\frac{\gamma_c^2}{4} + \omega_b^2}\right) \tag{A.10}$$

Note that $Q < 1$. The resonance ω_c will blue shift in this imperfect cavity.

AUTHOR INFORMATION

Corresponding Authors

John P. Philbin − *Harvard John A. Paulson School of Engineering and Applied Sciences, Harvard University, Cambridge, Massachusetts 02138, United States;* orcid.org/0000-0002-8779-0708; Email: jphilbin01@gmail.com

Yu Wang − *Department of Chemistry, School of Science, Westlake University, Hangzhou 310024 Zhejiang, China; Institute of Natural Sciences, Westlake Institute for Advanced Study, Hangzhou 310024 Zhejiang, China;* Email: wangyu19@westlake.edu.cn

Prineha Narang − *Harvard John A. Paulson School of Engineering and Applied Sciences, Harvard University, Cambridge, Massachusetts 02138, United States;* orcid.org/0000-0003-3956-4594; Email: prineha@seas.harvard.edu

Wenjie Dou − *Department of Chemistry, School of Science, Westlake University, Hangzhou 310024 Zhejiang, China; Institute of Natural Sciences, Westlake Institute for Advanced Study, Hangzhou 310024 Zhejiang, China; Department of Physics, School of Science, Westlake University, Hangzhou 310024 Zhejiang, China;* orcid.org/0000-0001-5410-6183; Email: douwenjie@westlake.edu.cn

Complete contact information is available at: https://pubs.acs.org/10.1021/acs.jpcc.2c04741

https://doi.org/10.1021/acs.jpcc.2c04741
J. Phys. Chem. C XXXX, XXX, XXX−XXX

Notes

The authors declare no competing financial interest.

■ ACKNOWLEDGMENTS

J.P.P. and Y.W. contributed equally to this manuscript. This work was primarily supported by the Department of Energy, Photonics at Thermodynamic Limits Energy Frontier Research Center, under Grant No. DE-SC0019140. J.P.P. also acknowledges support from the Harvard University Center for the Environment with calculations on the National Energy Research Scientific Computing Center (NERSC), a U.S. Department of Energy Office of Science User Facility operated under Contract No. DE-AC02-05CH11231. P.N. acknowledges support as a Moore Inventor Fellow through Grant No. GBMF8048 and gratefully acknowledges support from the Gordon and Betty Moore Foundation. Y.W and W.D. acknowledge support from Westlake University.

■ REFERENCES

(1) Thomas, A.; George, J.; Shalabney, A.; Dryzhakov, M.; Varma, S. J.; Moran, J.; Chervy, T.; Zhong, X.; Devaux, E.; Genet, C.; et al. Ground-State Chemical Reactivity under Vibrational Coupling to the Vacuum Electromagnetic Field. *Ang. Chem. Int. Ed.* **2016**, *128*, 11634−11638.

(2) Thomas, A.; Lethuillier-Karl, L.; Nagarajan, K.; Vergauwe, R. M. A.; George, J.; Chervy, T.; Shalabney, A.; Devaux, E.; Genet, C.; Moran, J.; et al. Tilting a ground-state reactivity landscape by vibrational strong coupling. *Science* **2019**, *363*, 615−619.

(3) Nagarajan, K.; Thomas, A.; Ebbesen, T. W. Chemistry under Vibrational Strong Coupling. *J. Am. Chem. Soc.* **2021**, *143*, 16877−16889.

(4) Lather, J.; Bhatt, P.; Thomas, A.; Ebbesen, T. W.; George, J. Cavity Catalysis by Cooperative Vibrational Strong Coupling of Reactant and Solvent Molecules. *Ang. Chem. Int. Ed.* **2019**, *58*, 10635−10638.

(5) Wiesehan, G. D.; Xiong, W. Negligible rate enhancement from reported cooperative vibrational strong coupling catalysis. *J. Chem. Phys.* **2021**, *155*, 241103.

(6) Imperatore, M. V.; Asbury, J. B.; Giebink, N. C. Reproducibility of cavity-enhanced chemical reaction rates in the vibrational strong coupling regime. *J. Chem. Phys.* **2021**, *154*, 191103.

(7) Mandal, A.; Li, X.; Huo, P. Theory of vibrational polariton chemistry in the collective coupling regime. *J. Chem. Phys.* **2022**, *156*, 014101.

(8) Ruggenthaler, M.; Flick, J.; Pellegrini, C.; Appel, H.; Tokatly, I. V.; Rubio, A. Quantum-electrodynamical density-functional theory: Bridging quantum optics and electronic-structure theory. *Phys. Rev. A* **2014**, *90*, 012508.

(9) Flick, J.; Ruggenthaler, M.; Appel, H.; Rubio, A. Atoms and molecules in cavities, from weak to strong coupling in quantum-electrodynamics (QED) chemistry. *Proc. Natl. Acad. Sci. U. S. A.* **2017**, *114*, 3026−3034.

(10) Flick, J.; Narang, P. Cavity-Correlated Electron-Nuclear Dynamics from First Principles. *Phys. Rev. Lett.* **2018**, *121*, 113002.

(11) Fregoni, J.; Granucci, G.; Coccia, E.; Persico, M.; Corni, S. Manipulating azobenzene photoisomerization through strong light-molecule coupling. *Nat. Commun.* **2018**, *9*, 4688.

(12) Flick, J.; Narang, P. Ab initio polaritonic potential-energy surfaces for excited-state nanophotonics and polaritonic chemistry. *J. Chem. Phys.* **2020**, *153*, 094116.

(13) Haugland, T. S.; Ronca, E.; Kjønstad, E. F.; Rubio, A.; Koch, H. Coupled Cluster Theory for Molecular Polaritons: Changing Ground and Excited States. *Phys. Rev. X* **2020**, *10*, 041043.

(14) Deprince, A. E. Cavity-modulated ionization potentials and electron affinities from quantum electrodynamics coupled-cluster theory. *J. Chem. Phys.* **2021**, *154*, 094112.

(15) Schäfer, C.; Flick, J.; Ronca, E.; Narang, P.; Rubio, A. Shining Light on the Microscopic Resonant Mechanism Responsible for Cavity-Mediated Chemical Reactivity. *arXiv:2104.12429 [quant-ph]* **2021**, na.

(16) Pavosevic, F.; Hammes-Schiffer, S.; Rubio, A.; Flick, J. Cavity-Modulated Proton Transfer Reactions. *J. Am. Chem. Soc.* **2022**, *144*, 4995−5002.

(17) Campos-Gonzalez-Angulo, J. A.; Ribeiro, R. F.; Yuen-Zhou, J. Resonant catalysis of thermally activated chemical reactions with vibrational polaritons. *Nat. Commun.* **2019**, *10*, 4685.

(18) Li, T. E.; Nitzan, A.; Subotnik, J. E. On the origin of ground-state vacuum-field catalysis: Equilibrium consideration. *J. Chem. Phys.* **2020**, *152*, 234107.

(19) Li, X.; Mandal, A.; Huo, P. Cavity frequency-dependent theory for vibrational polariton chemistry. *Nat. Commun.* **2021**, *12*, 1315.

(20) Yang, P. Y.; Cao, J. Quantum Effects in Chemical Reactions under Polaritonic Vibrational Strong Coupling. *J. Phys. Chem. Lett.* **2021**, *12*, 9531−9538.

(21) Kéna-Cohen, S.; Yuen-Zhou, J. Polariton Chemistry: Action in the Dark. *ACS Cent. Sci.* **2019**, *5*, 386−388.

(22) Hertzog, M.; Wang, M.; Mony, J.; Börjesson, K. Strong light−matter interactions: a new direction within chemistry. *Chem. Soc. Rev.* **2019**, *48*, 937−961.

(23) Simpkins, B. S.; Dunkelberger, A. D.; Owrutsky, J. C. Mode-Specific Chemistry through Vibrational Strong Coupling (or A Wish Come True). *J. Phys. Chem. C* **2021**, *125*, 19081−19087.

(24) Dou, W.; Miao, G.; Subotnik, J. E. Born-Oppenheimer Dynamics, Electronic Friction, and the Inclusion of Electron-Electron Interactions. *Phys. Rev. Lett.* **2017**, *119*, 046001.

(25) Dou, W.; Subotnik, J. E. Perspective: How to understand electronic friction. *J. Chem. Phys.* **2018**, *148*, 230901.

(26) Wang, D. S.; Neuman, T.; Flick, J.; Narang, P. Llight-matter interaction of a molecule in a dissipative cavity from first principles. *J. Chem. Phys.* **2021**, *154*, 104109.

(27) Kramers, H. A. Brownian motion in a field of force and the diffusion model of chemical reactions. *Physica* **1940**, *7*, 284−304.

(28) Grote, R. F.; Hynes, J. T. The stable states picture of chemical reactions. II. Rate constants for condensed and gas phase reaction models. *J. Chem. Phys.* **1980**, *73*, 2715−2732.

(29) Pollak, E.; Grabert, H.; Hänggi, P. Theory of activated rate processes for arbitrary frequency dependent friction: Solution of the turnover problem. *J. Chem. Phys.* **1989**, *91*, 4073−4087.

(30) Sun, J.; Vendrell, O. On the Suppression and Enhancement of Thermal Chemical Rates in a Cavity. *J. Phys. Chem. Lett.* **2022**, *13*, 4441−4446.

(31) Lindoy, L. P.; Mandal, A.; Reichman, D. R. Resonant Cavity Modification of Ground State Chemical Kinetics. *J. Phys. Chem. Lett.* **2022**, *13* (28), 6580.

(32) Rokaj, V.; Welakuh, D. M.; Ruggenthaler, M.; Rubio, A. Light−matter interaction in the long-wavelength limit: no ground-state without dipole self-energy. *J. Phys. B Atom., Mol. Opt. Phys.* **2018**, *51* (3), 034005.

(33) Schäfer, C.; Ruggenthaler, M.; Rokaj, V.; Rubio, A. Relevance of the Quadratic Diamagnetic and Self-Polarization Terms in Cavity Quantum Electrodynamics. *ACS Photonics* **2020**, *7*, 975−990.

(34) Dou, W.; Nitzan, A.; Subotnik, J. E. Frictional effects near a metal surface. *J. Chem. Phys.* **2015**, *143*, 054103.

(35) Nitzan, A. *Chemical Dynamics in Condensed Phases: Relaxation, Transfer, and Reactions in Condensed Molecular Systems*; Oxford University Press, 2006; pp 1−744.

(36) Hänggi, P.; Talkner, P.; Borkovec, M. Reaction-rate theory: Fifty years after Kramers. *Rev. Mod. Phys.* **1990**, *62*, 251−341.

https://doi.org/10.1021/acs.jpcc.2c04741
J. Phys. Chem. C XXXX, XXX, XXX−XXX